



## Enhancement strategy of polyethersulfone (PES) membrane by introducing pluronic F127/graphene oxide and phytic acid/graphene oxide blended additives: preparation, characterization and wastewater filtration assessment

Fateme Kouhestani<sup>a</sup>, Mohamad Ali Torangi<sup>b,\*</sup>, Alireza Motavalizadehkakhky<sup>a</sup>,  
Reza Karazhyan<sup>c</sup>, Rahele Zhiani<sup>d</sup>

<sup>a</sup>Department of chemistry, Neyshabur Branch, Islamic Azad University, Neyshabur, Iran,  
emails: Fateme\_kouhestany@yahoo.com (F. Kouhestani), Amotavalizadeh@yahoo.com (A. Motavalizadehkakhky)

<sup>b</sup>Department of Polymer Engineering, Faculty of Engineering, Golestan University, Gorgan, Iran, email: m.torangi@gu.ac.ir

<sup>c</sup>Industrial Biotechnology on Microorganisms Department, ACECR, Mashhad, Iran, email: Reza\_karazhyan2002@yahoo.com

<sup>d</sup>Department of chemistry, Islamic Azad University, Neyshabur Branch, Young and Elite Research Club, Neyshabur, Iran,  
email: R\_zhiani2006@yahoo.com

Received 12 March 2019; Accepted 5 August 2019

### ABSTRACT

In this study hydrophilic modification of polyethersulfone (PES) membrane was achieved through the blending of pluronic F127 (PF-127)/graphene oxide (GO) and phytic acid (PA)/GO blended additives. The modified PES membranes were prepared using an immersion precipitation technique. The membrane's characteristics were evaluated using scanning electron microscopy, Fourier-transform infrared spectroscopy, atomic force microscopy, water contact angle, tensile testing and dynamic test of oily wastewater treatment. The modification of GO by PF-127 and PA improved the dispersibility of GO in the PES polymer matrix, so it can highly affect the morphology, filtration performance and fouling mitigation of membrane. According to the results, a substantial increase in mechanical properties was observed for the (PF-127/GO; 6 wt.)/PES and (PA/GO; 4 wt.)/PES membranes. It was revealed that by adding modified GO, because of increasing surface hydrophilicity, the flux increased from 121.1 Lm<sup>-2</sup> h<sup>-1</sup> for neat PES membrane to 258.2, 303 Lm<sup>-2</sup> h<sup>-1</sup> for (PF-127/GO; 6 wt.)/PES, (PA/GO; 4 wt.)/PES membranes respectively. In addition, the results of the permeability recovery ratio showed that the anti-fouling properties of the modified PES membranes were improved due to the increase in membrane surface hydrophilicity.

*Keywords:* Polyethersulfone; Membrane; Phytic acid; Pluronic F127; Graphene oxide

### 1. Introduction

Nanofiltration (NF) technology has now become an attractive option for the treatment and reuse of industrial and municipal wastewaters [1]. One of the main problems associated with this technology is membrane fouling. The NF performance inevitably decreases with filtration time due to this problem especially when hydrophobic membranes

are used in the separation. Polyethersulfone (PES) is one of hydrophobic polymers which is used in the commercial membrane manufacturing. It possesses excellent chemical resistance, environmental endurance as well as easy processing, thermal and mechanical properties [2–4]. Despite these desirable properties, PES has disadvantages. The main disadvantage of the PES is related to the hydrophobicity character of it which has restricted its usage in separation processes [5,6]. The inherent hydrophobicity of PES due

\* Corresponding author.

to its structure leads to a low membrane flux and is easily susceptible to fouling [4,7]. Therefore, efforts have devoted to improving the hydrophilicity of PES either by chemical or physical modifications. These modifications of PES have been reported in the literature. Some of these modifications are blending with hydrophilic nanoparticles [8], the addition of additives [9,10], surface grafting polymerization [11], coating with hydrophilic polymers [12] and so on. Among various nanomaterials, graphene-based nanomaterials have been considered for different fields of technology and science due to their unique properties, including excellent thermal properties, mechanical and chemical stability, high surface area, and low-cost production [13]. Graphene oxide (GO), with a hydrophilic feature, due to the presence of oxygenated functional groups like epoxy, hydroxyl, carboxyl and carbonyl groups on its structure, has been applied for polymeric membrane modification [14]. Since many studies have been conducted on membrane modifications using GO [15–17]. One challenge in designing and fabricating hybrid membranes containing GO is introducing increased GO with homogeneous distribution into the polymer matrix. The presence of, hydroxyl, epoxies groups on the surface and carboxyl, carbonyl groups at the edges of GO enable it to be dispersed in the polar solvent [18]. So to improve the dispersion of GO in organic solvents and better compatibility with polymer matrices, the GO must be modified by suitable agents.

For GO dispersity in the non-polar medium, lots of studies have been conducted. Yu and Xie [19] used a phase transfer method for dispersion of GO in the *n*-octane solvent. For this purpose, he applied oleylamine as a suspending agent in a solvent. Consequently, a strong interaction was formed between oleylamine and GO.

As a modification agent, pluronic F127 (PF-127) is an amphiphilic surfactant with a chemical composition of poly(ethylene oxide)<sub>98</sub> – poly(propylene oxide)<sub>67</sub> – poly(ethylene oxide)<sub>98</sub> (PEO<sub>98</sub> – PPO<sub>67</sub> – PEO<sub>98</sub>) that can be added to GO [19]. The presence of the alkyl chain in PPO can prevent reagglomeration of graphene in non-polar solution [20]. On the other hand, the presence of PF-127 in membrane structure can effectively increase the hydrophilic of the membrane and improve the membrane fouling resistance. The long PEO segments give PF-127 the excellent ability to reduce hydrophobic compounds adsorption and the PPO segment with the appropriate length makes the PF-127 located in the membrane matrix stable [21].

One of the other amphiphilic agents that can be used in GO modification is phytic acid (PA). PA, composed of six phosphate groups, exhibits an excellent characteristic for the modification of numerous materials [22]. The prepared PA/GO blended additive has amphiphilic properties because it has hydrophobic aromatic domains and hydrophilic functional groups such as inositol triphosphate and phosphoric acid [23]. Therefore, this additive can form a strong  $\pi$ -stacking interaction with some organic solvents and is a good candidate for the GO modifier agent. In this work, to improve the hydrophilic and morphological properties of the PES membrane, the GO that has been modified by pluronic F127 and PA was added into the membrane. The effects of the modified additive and PES concentrations on morphology, mechanical properties, hydrophilicity and permeation flux of the PES membranes were investigated.

## 2. Experimental setup

### 2.1. Materials

PES (Ultrason E6020 P, MW = 58,000 g mol<sup>-1</sup>) was purchased from BASF Chemical Co. (Germany) and was dried at 110°C for 12 h before use. The solvent of N,N-dimethylacetamide (DMAc) with an analytical purity of 99.5% was supplied from Merck (Germany). Triblock copolymer pluronic F127 (PF-127) (PEO<sub>100</sub>-PPO<sub>65</sub>-PEO<sub>100</sub>) (MW = 12.6 kg mol<sup>-1</sup>; PEO weight content, %PEO = %70) was purchased from Sigma-Aldrich (St. Louis, MO, United States). GO purchased by the company Abalonyx AS (Norway-OSLO). PA was obtained from Sigma-Aldrich. All other chemicals were of commercial analytical grade. Wastewater used in the present study was sampled from a local grease factory. Three pollution indices of the oily wastewater, that is, turbidity, chemical oxygen demand (COD), and total dissolved solids (TDS) were in the range of 332 NTU, 3,012 and 1,211 mg L<sup>-1</sup>, respectively.

### 2.2. Modification of GO

In this work, a typical experiment to modified GO was performed by a hydrothermal method. In this typical procedure, 60 mg of PF127 was dispersed in 100 ml deionized water at room temperature for 24 h. The homogenous solution is then added slowly to 25 mL of GO water solution (5 mg mL<sup>-1</sup>). After 24 h of vigorous stirring, the suspension was transferred to a teflon-lined stainless steel sealed vessel and heated to 180°C for 12 h. Then the mixtures were cooled to room temperature overnight. The product was washed with ethanol and water several times and then freeze-dried under vacuum condition for 24 h.

The PA/GO was prepared using the same method and the mass ratio of GO and PA was 1:5.

### 2.3. Membrane preparation

Asymmetric membranes of modified PES membranes were prepared using the phase inversion method induced by immersion precipitation. At first, various loading of 0, 2, 4, 6 and 8 wt.% modified GO were dissolved into the DMAc and was sonicated at 25°C for 48 h to obtain a uniform and homogeneous casting suspension. Subsequently, 21 wt.% PES was added and the mixture was sonicated again for 3 d till completely transparent mixture was obtained. After degassing, this mixture poured onto a glass plate and spread with a membrane applicator to be as thin as 250  $\mu$ m at room temperature. The nascent membrane was evaporated at 25°C  $\pm$  1°C for 15 s and then immersed in the water coagulation bath maintained at 25°C  $\pm$  1°C for at least 2 d to completely remove the remained solvent before characterization.

### 2.4. Thermodynamic stability aspect of membrane formation

To predict the effect of the polymer solution and non-solvent on thermodynamic of phase separation, ternary phase diagrams were determined. The ternary phase diagram is useful for the prediction of the phase transitions that cloud occur when phase separation is induced according to the immersion precipitation method [24].

The ternary phase diagram of (modified GO/PES)/solvent/non-solvent systems at ambient temperature, which are constructed based on the cloud-point measurements. Hence, cloud-point data were obtained by the titration method and was obtained as follows: (modified GO/PES) solution with different composition was taken into a glass-ware and the non-solvent was slowly added to the modified GO/PES solution from a burette while the glass-ware was subjected to gentle stirring until the clear polymer solution visually became too cloudy. The composition at the cloud point was then calculated from the weight of the added non-solvent, solvent, and polymer in the glass-ware.

### 2.5. Characterization of GO, PF-127/GO and PA/GO

The morphology images of GO, PF-127/GO, and PA/GO were captured with scanning electron microscopy (SEM) (KYKY EM3200, Japan). Besides, the Fourier-transform infrared (FTIR, Thermo Nicolet 6700, USA) spectroscopy was employed to analyze the composition of GO, PF-127/GO and PA/GO.

### 2.6. Membrane characterizations

The cross-sectional morphologies of the membranes were characterized using the KYKY EM3200 instrument (Japan) with an accelerating voltage of 20 kV. For the preparation of the cross-sectional images, the dried membrane samples were immersed in liquid nitrogen and then fractured. The membranes were then coated with a thin film of gold by a gold sputter coater (Cressington 108 auto, UK).

The hydrophilicity of the membrane top surface was characterized based on a water contact angle measuring system (G10, KRUSS, Germany). For this purpose, de-ionized water was used as the probe liquid in all the measurements. Measuring system equipped with video capture at room temperature. To minimized experimental error, the contact angles were measured five times for each sample and then were averaged.

Atomic force microscopy (AFM) was used to analyze the surface morphology and roughness of the prepared membranes. The AFM device was a DualScope™ scanning probe-optical microscope (DME model C-26, Switzerland). Small squares of the prepared membranes (approximately 1 cm<sup>2</sup>) were cut and glued on the glass substrate. The membrane surfaces were imaged in a scan size of 5 μm × 5 μm by DME SPM software.

The structural changes were assessed by FTIR using a Thermo Scientific Nicolet 6700 FTIR spectrometer (United States). FTIR is used to obtain the infrared spectrum for a particular sample. It collects data over a wide spectral range and this data can be used to identify specific functional groups that are present in the sample being studied. Spectral outputs were recorded in transmittance mode as a function of wave number.

Tensile testing to study tensile strength, tensile modulus and elongation at break (mm) were performed using SANTAM 20KN (Iran) testing machine at ambient temperature. All tests were done according to ASTM D638 standard [25]. The samples were analyzed at a cross-head speed of 1 mm min<sup>-1</sup>. The film specimens had a dimension

of 60 mm × 10 mm × 0.25 mm. The grip distance was 50 mm and the gage length was 25 mm. Property reported values here to represent an average of the results for tests run on three specimens.

### 2.7. Experimental procedure

The laboratory experiments are carried out in the cross-flow filtration unit [26] at ambient temperature and trans-membrane pressure of 10 bar. At the beginning of the process, the membranes are subjected to pure water permeability for assessing their functions and operational evaluations. After pure water filtration, the feed reservoir was emptied and refilled with the feed solution to its filtration. This solution was forced to permeate through the membrane at the same pressure for 30 min and the flux was recorded. To evaluate the filtration efficiency in the removal of pollution indices of COD, TDS, and turbidity of the wastewater, their values in the feed and permeate were measured. The COD was measured by using the thermoreactor of ET-108 (Aqualytic, Germany) for the heating and digestion of COD vials contents along with the MD 200 COD photometer from Lovibond Tintometer (Germany). Conductivity meter (model 666 222, LEYBOLD, Germany) was used for measuring the TDS. The turbidity meter (model 2020WE, USA) was used to measure the turbidity.

The solute rejection was measured at 10 bar and calculated by Eq. (1) [27]:

$$R(\%) = \left( 1 - \frac{C_p}{C_f} \right) \times 100\% \quad (1)$$

where  $C_p$  and  $C_f$  are the concentration of pollution indices in permeate and feed solutions, respectively.

### 2.8. Membrane fouling analysis

The degree of membrane fouling was calculated quantitatively using the resistance-in-series model [4]:

$$J = \frac{\text{TMP}}{\eta \times R_t} \quad (2)$$

where  $J$  is the permeation flux (Lm<sup>-2</sup> h<sup>-1</sup>); TMP = trans-membrane pressure (10 bar);  $\eta$  = viscosity of water at room temperature.  $R_t$  is the total resistance and calculated as:

$$R_t = R_m + R_f + R_c \quad (3)$$

where  $R_m$  is the membrane hydraulic resistance,  $R_f$  is the sum of the resistances caused by solute adsorption into the membrane pores or walls and chemically reversible cake.  $R_c$  is the cake resistance formed by the cake layer deposited over the membrane surface. Resistances values were calculated by the following equations:

$$R_m = \frac{\text{TMP}}{\eta \times j_{iw}} \quad (4)$$

$$R_f = \frac{\text{TMP}}{\eta \times j_{i_w}} - R_m \quad (5)$$

$$R_c = \frac{\text{TMP}}{\eta \times J} - (R_m + R_f) \quad (6)$$

$j_{i_w}$  is the pure water flux at the beginning of the process (before wastewater filtration) and used to determine the  $R_m$ . After wastewater filtration, the membrane was perfectly washed in a cross-flow manner with distilled water and pure water flux ( $j_{i_w}$ ) was measured again for using to determine the  $R_f$ .

### 3. Results and discussion

#### 3.1. Thermodynamic stability of ternary (modified GO/PES)/DMAs/Water

Thermodynamic analysis reveals the effect of interaction potentials on the mixing and demixing of blended components, which are often demonstrated by phase diagrams [24]. The ternary phase diagram of the (modified GO/PES)/DMAs/Water combination systems are obtained from the cloud points measurements which are shown in Fig. 1. As can be seen, by increasing water concentration, the cloud point curve shifts closer to the (modified GO/PES)/DMAs axis because of the lower stability of the polymer solution. This phenomenon indicates that the phase separation process is eventually dominated by the liquid–liquid demixing. On the other hand, blending modified GO into the polymer solution reduces the thermodynamic stability and can promote phase inversion. This might be explained by the fact that the hydrophilic nature of the PF-127 and PA causes water inflow into the nascent membrane.

The gelation boundary for the (PA/GO)/PES/DMAs/water system is closer to the (modified GO/PES)/DMAs axis as compared to the other (PF-127/GO)/PES/DMAs/water systems. This result is due to the higher affinity of PA to water than PF-127 which results in faster liquid–liquid demixing.

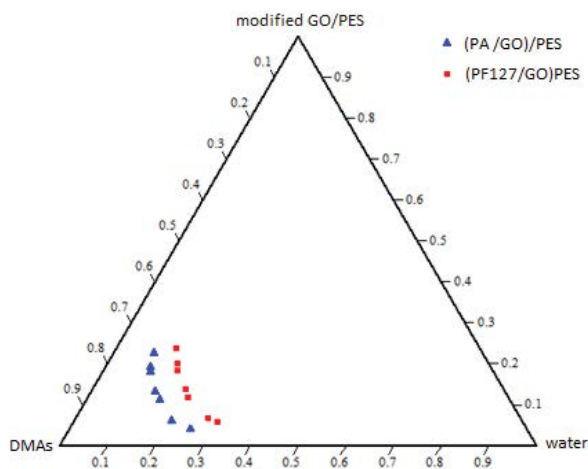


Fig. 1. Ternary phase diagram of (modified GO/PES)/DMAs/water system.

#### 3.2. Morphology of GO, PF-127/GO and PA/GO

The morphologies of GO, PF-127/GO and PA/GO were characterized by SEM as shown in Fig. 2. The SEM images of GO revealed that the surface of GO was smooth which was corresponding to its layered-like structure but all PF-127/GO and PA/GO composites exhibit three-dimensional porous structures, formed during the hydrothermal process. It can be observed that the PF-127/GO presented a honeycomb-like structure and uniform distribution due to the deformation of GO layers by strong  $\pi$ - $\pi$ -stacking. The SEM image of PA/GO represents a micropore structure which is attributed to the fact that each PA molecule can interact with several GO sheets to form a branched microstructure.

#### 3.3. Morphology of membranes

In order to understand the influence of modified GO on the membrane structure, cross-section of the membranes was observed using SEM (Fig. 3). As can be seen, all membranes exhibit an asymmetric structure consisting of two sections, that is, a dense top-layer and a porous sublayer and there is no significant difference between the modified and unmodified membrane's structure. However, it is clear that the addition of PF-127 and PA to GO significantly affected the finger-like pore size and the connectivity of the pores between the sub-layer and top layer of the PES membranes. Generally, structures with large pores depend on the rate difference between the diffusion rate of non-solvent to casting solution and the pervasion rate of the solvent to the coagulation bath [7]. The hydrophilic nature of two additives causes a great diffusion velocity of water into the nascent membrane during the phase inversion so macrovoids grow throughout the membrane. In fact, uniform distribution of GO in casting solution due to the presence of additives leads to the more regular formation of macrovoids in the membrane.

The presence of PF-127 and PA has an important effect on the micelle structure of the casting solution. The volume and density of the micelles in the casting solution influence on the membrane structure. By increasing PF-127 (up to 6 wt.%) and PA (up to 4 wt.%), the density and size of micelles increases, so membranes with dense skin layer, the porous sublayer, and the macroporous support layer will be formed. When the concentrations of PF-127 and PA increase more than a certain value (>6 wt.% for PF-127 and >4 wt.% for PA) the sublayer gradually thickened into a dense sponge-like structure, the finger-like holes of support layer became larger and gradually extended to the bottom of the membrane. In fact, with increasing additives concentration in casting solution the viscosity greatly increases and the movement of macromolecules is suppressed. So the liquid–liquid demixing process is delayed and the phase separation process is dominated by the solid–liquid demixing. Comparison between (PF-127/GO)/PES and (PA/GO)/PES membranes indicate that the membranes modified by PA/GO are more porous than other membranes modified by (PF-127/GO). It is justifiable by greater hydrophilicity of PA due to the six phosphates groups attached symmetrically to a cyclohexanehexol ring which is liable to interact with water molecules.

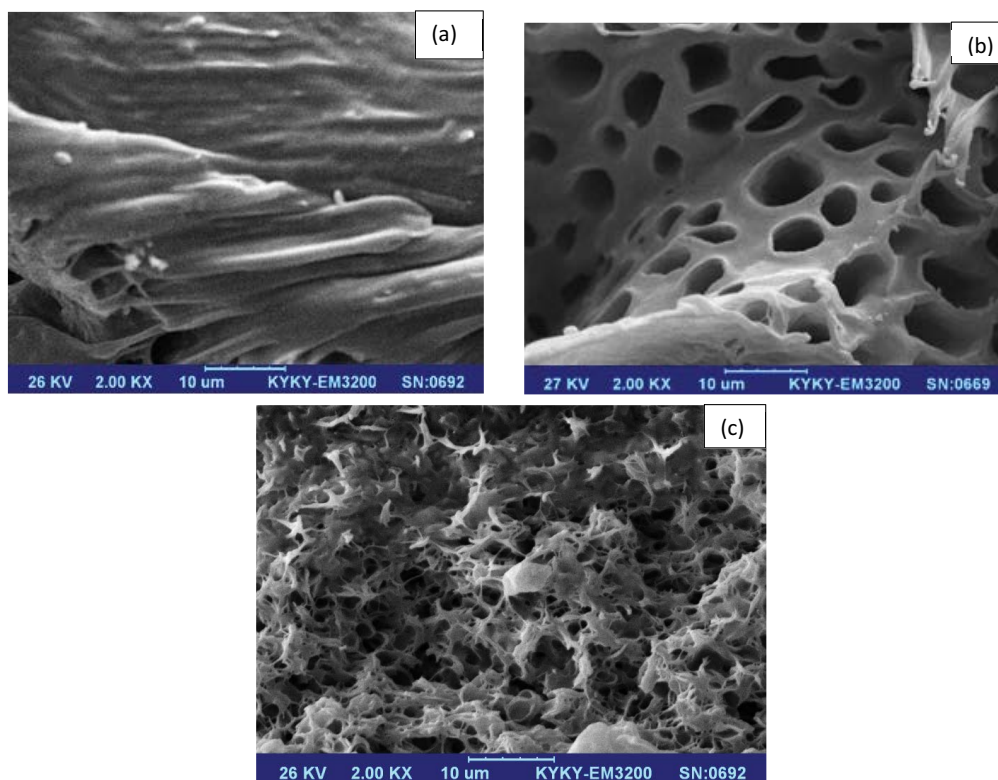


Fig. 2. SEM images of (a) GO, (b) PF-127/GO, and (c) PA/GO.

### 3.4. Mechanical properties of membranes

Table 1 shows the effect of the modified GO incorporation on the essential mechanical properties of the membranes. Generally, GO is used in polymeric matrices to improve the thermal, electrical and mechanical properties. Whereas it has high values of mechanical properties in polymeric matrices, this matter can be an increasing agent of matrix stiffness [28]. As mentioned to improve the dispersion of GO in DMAc solvent and better compatibility with polymer matrices, the GO is modified by PF-127 and PA additives. The uniform distribution of GO in polymer matrix can be prompts the mechanical property of the membrane. As can be seen, the tensile modulus and strength sequentially enhanced with increasing the modified GO content up to certain values. Afterward, an excessive amount of modified GO more than a certain concentration is leading to an insignificant increase in the membrane's tensile strength and Young's modulus. The GO modification significantly achieved the homogeneous dispersion in the PES matrix that improved interfacial adhesion between GO particles and the polymer matrix. On the other hand, the free motion of polymeric chains is partly restricted by the intermolecular forces between the polymeric chains and the GO dispersed uniformly in a polymer.

By increasing modified GO content (more than 6 wt.% for PF-127/GO and 4 wt.% for PA/GO) the static hindrance and coalesces of modified GO in the membrane may wreck

the crystallinity and thus decrease the tensile strength and Young's modulus.

In particular, the membranes containing 6 wt.% of PF-127/GO and 4 wt.% for PA/GO showed the highest moduli and tensile strength that were much higher than that of PES itself while showing strengths comparable to that of neat PES membrane.

Also, the elongation at break was reasonably decreased with increasing values of modified GO content more than 4 wt.% of both modified GO due to the strong interaction between the modified GO and the polymer, which restricts the movement of the polymer chains. PES membranes modified with PA/GO are more porous than those of modified with PF-127/GO. So these membranes have relatively less mechanical properties due to more porosity than others.

### 3.5. Contact angle measurement

Water contact angle measurement was conducted to investigate the hydrophilicity and surface wettability of the membranes. It can also be seen from Fig. 4 that the water contact angle of the membranes decreases with an increase in the amount of modified GO (0–4 wt.%). However, a higher amount of the modified GO ( $\geq 4$  wt.%) leads to an increase in the water contact angle of the membranes. The membrane hydrophilicity is improved by the addition of modified GO due to the presence of affinity and interaction between PF-127

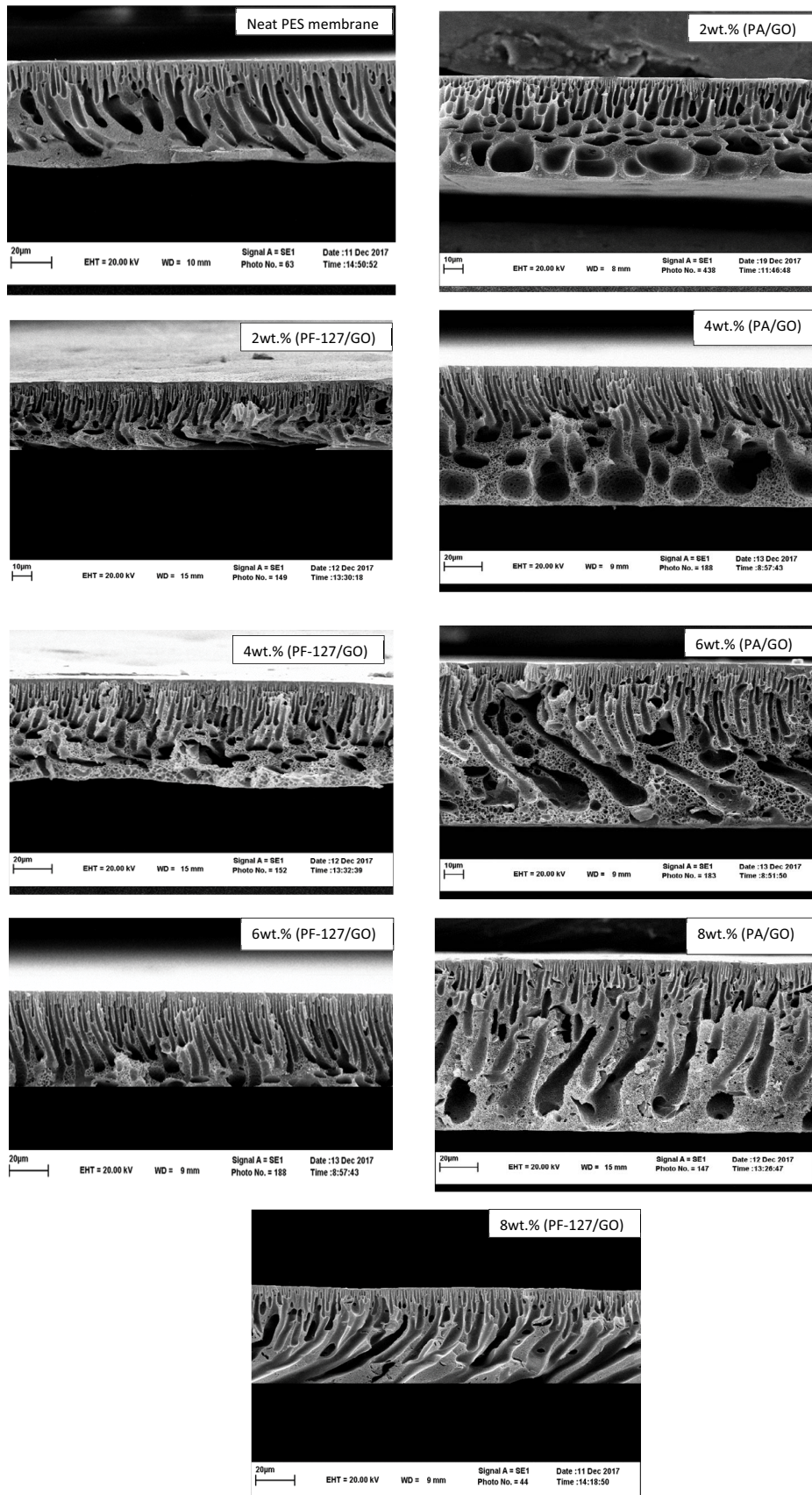


Fig. 3. SEM cross-sectional images of the PES membranes modified with PF-127/GO and PA/GO.

Table 1  
Mechanical properties of the PES membranes modified with PF-127/GO and PA/GO

Membrane	Tensile strength (MPa)	Young's modulus (MPa)	Elongation at break (mm)
Neat PES membrane	2.75	53	0.5
(PF-127/GO; 2 wt.)/PES	3.7	69	1.87
(PF-127/GO; 4 wt.)/PES	4.5	86	2.65
(PF-127/GO; 6 wt.)/PES	4.7	89	2.1
(PF-127/GO; 8 wt.)/PES	3	73	1.3
(PA/GO; 2 wt.)/PES	3.5	61	1.67
(PA/GO; 4 wt.)/PES	3.7	66	1.95
(PA/GO; 6 wt.)/PES	2.6	50	1.4
(PA/GO; 8 wt.)/PES	2.2	41	0.94

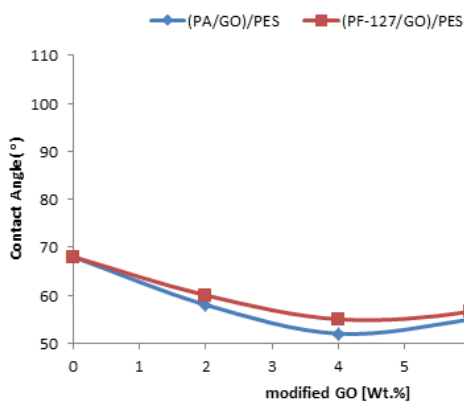


Fig. 4. Contact angle of PES membranes modified with PF-127/GO and PA/GO.

and PA as additives that used to GO modification and coagulant (water) which provides a great migration of hydrophilic GO functional groups toward membrane surface results in membrane hydrophilicity enhancement and reduction of interface energy with water. The higher modified GO content ( $\geq 4$  wt.%) will lead to a decrease in hydrophilicity due to the high density, aggregation of the modified GO inside the polymeric matrix, irregular placement of modified GO in membrane structure and consequently reduction of hydrophilic functional groups on the membrane [29]. Also, all PES membranes modified by PA/GO have a lower contact angle than others. It can be attributed to the stronger affinity of PA than PF-127 due to the six phosphates groups attached symmetrically to a cyclohexanehexol ring to water molecules.

### 3.6. AFM analysis

AFM images of the neat and modified PES membranes are shown in Fig. 5. These images confirm that the neat PES membrane has a smoother structure than the modified membranes with PF-127/GO and PA/GO. The surface roughness parameters of membranes in scan areas of  $5 \mu\text{m} \times 5 \mu\text{m}$  were calculated by DME SPM software and are presented in Table 2. For PES membranes that modified with PF-127/GO the Ra value of the neat membrane was about 20.36 nm whereas these values in samples containing 6 wt.% PF-127/GO

reached 41.4 nm. When the content of the PF-127/GO was increased to 8 wt.%, the surface roughness of the PES membrane decreased. It might be explained by that the PEO part of PF-127 has lower miscibility than PPO part to PES; thus, it tends to separate from the hydrophobic PES polymer and PPO and then locates the membrane surface. Therefore the surface pores of the membranes were occupied by these organic groups consequently the surface smoothness increased gradually [30]. In the case of (PA/GO)/PES membranes, modified membranes presented rougher surface than PES without PA/GO adding and the pores of prepared membranes became more visible with an increase of PA/GO content up to 4 wt.%. Because the bulk density of PES is estimated to be  $1.38 \text{ g mL}^{-1}$  and the bulk density of PA is  $1.43 \text{ g mL}^{-1}$ , gravity has more effect on PA than PES. So, it is not observed the PA on the membrane surface due to the main gravity role. By adding more PA/GO ( $>4$  wt.%) in the matrix, the roughness decreased due to the increase in viscosity of casting solution and aggregation of PA/GO and finally blocking the pores.

The Ra of the neat and (PA/GO; 4 wt.)/PES membranes were 28.36 and 40.1 nm, respectively. Higher roughness commonly led to two changes in the modified membrane; an increase of efficient filtration area and a decrease of the anti-fouling performance. The root mean squared (RMS) is the root mean square average of height deviations taken from the mean data plane. Membrane surface roughness data that examined in terms of the RMS and the mean surface roughness (Ra) are shown in Table 2.

### 3.7. FTIR analysis

Fig. 6 shows the FTIR spectrum of GO, PF-127, PF-127/GO, PA, PA/GO, PES and modified PES membranes. This analysis was conducted to observe the compositions and to identify the functional groups of membranes upon the introduction of PF-127/GO and PA/GO.

The GO represents characteristic C=O stretching vibration at  $1,730 \text{ cm}^{-1}$ , C–OH stretching vibration at  $\sim 1,230 \text{ cm}^{-1}$ , C–O stretching vibration at  $\sim 1,040 \text{ cm}^{-1}$  for the epoxy group, O–H stretching vibration at  $3,435 \text{ cm}^{-1}$ , and skeletal vibration of unoxidized graphitic domains at  $1,620 \text{ cm}^{-1}$ . FTIR spectrum of PF-127 is characterized by principal absorption peaks at  $2,884 \text{ cm}^{-1}$  (C–H, stretch, aliphatic),  $1,342 \text{ cm}^{-1}$  (in-plane O–H bend) and  $1,111 \text{ cm}^{-1}$  for C–O stretch.

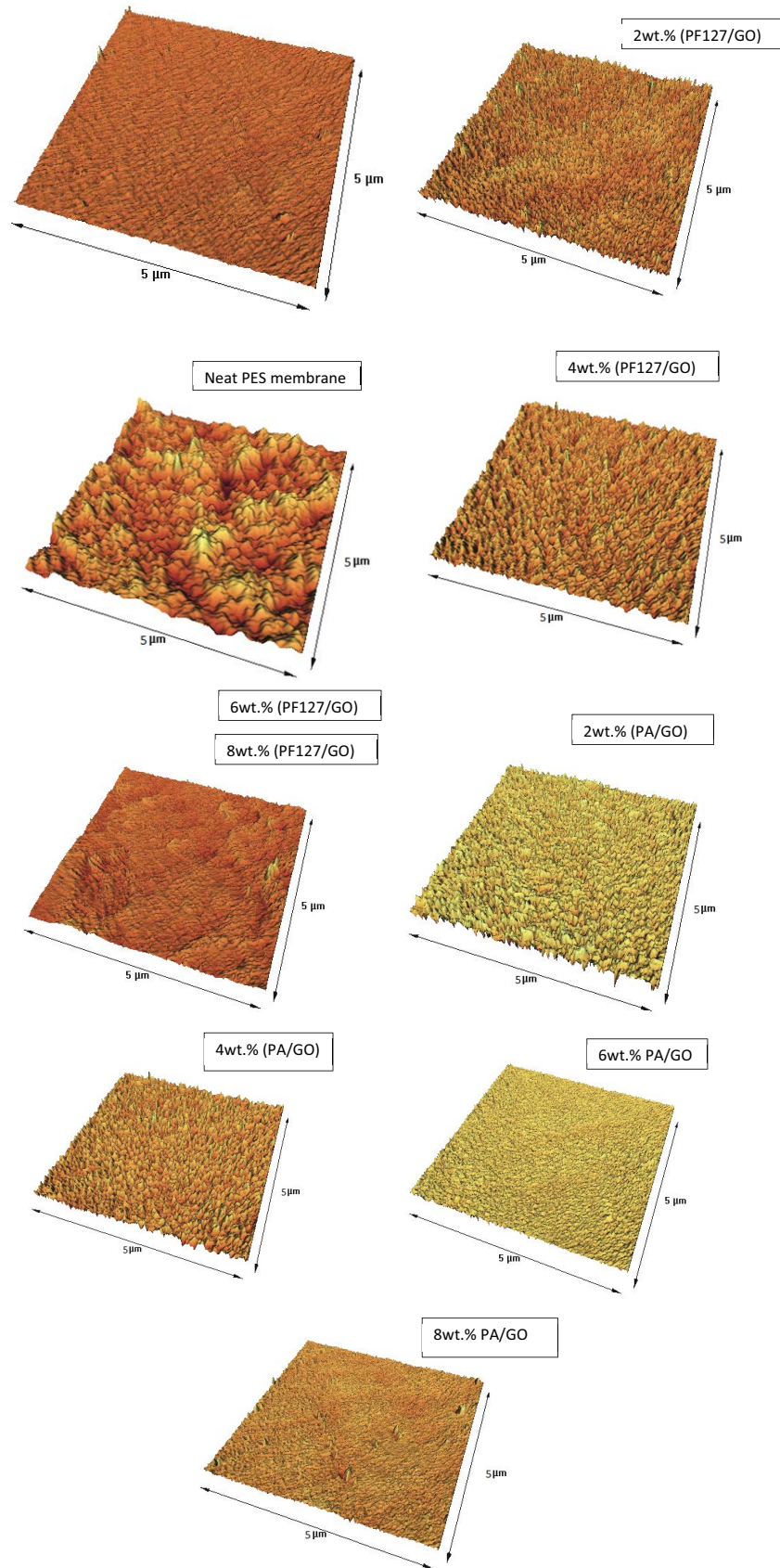


Fig. 5. AFM three-dimensional surface images of PES membranes modified with PF-127/GO and PA/GO.

The characteristic bands for PA at 3,400 assigned as (O–H) group, 1,638 and 1,150  $\text{cm}^{-1}$  attributed to phosphate hydrogen group, 500 and 1,005  $\text{cm}^{-1}$  related to the phosphate group.

There are several characteristic bands of PES membrane that can be identified including aromatic C=C band at 1,450 and 1,580  $\text{cm}^{-1}$ , aromatic ether (–C–O–C–) at 1,240  $\text{cm}^{-1}$  and

asymmetric/symmetric stretching of O=S=O at 1,320 and 1,162  $\text{cm}^{-1}$ .

The FTIR of PF-127/GO illustrates peaks at 1,733 and 1,222  $\text{cm}^{-1}$  that are attributed to C=O and C–O, respectively, while the peak appearing at 1,582  $\text{cm}^{-1}$  corresponds to the deformed C–C bond because of the existence of epoxy groups.

The FTIR spectrum of the prepared (PA/GO)/PES exhibits its characteristic bands around 3,600 and 3,420 from the OH stretching vibration indicating the presence of a hydrophilic layer on the surface and presence of phosphate hydrogen group the modified membrane which confirms the proper embedment of the GO/PA into the PES matrix. OH group in FTIR spectra of (GO/PA)/PES indicates the presence of oxygenized functional groups in the modified PES matrix which was created by the hydrogen interactions of GO carboxyl groups and O=S=O groups of PES.

In the case of (PF-127/GO)/PES, there are some featured peaks in modified PES membranes, of which the peak at 3,530  $\text{cm}^{-1}$  is due to O–H stretching vibration and the peak at 1,654  $\text{cm}^{-1}$  may be ascribed to the bonding vibration of C=C and C=O in GO. Also, the characteristic peaks of PF-127 in blend membranes were overlapped by PES peaks with the high relative intensity of the C–O bond appearing at 1,107  $\text{cm}^{-1}$ .

Table 2

Roughness parameters of membrane surface calculated with DME SPM software

Membrane	$R_a$ (nm)	RMS (nm)
Neat PES membrane	20.361	12.02
(F-127/GO; 2 wt.%)/PES	34.732	22.82
(F-127/GO; 4 wt.%)/PES	39.1	25.6
(F-127/GO; 6 wt.%)/PES	41.4	28.4
(F-127/GO; 8 wt.%)/PES	26.5	16.6
(PA/GO; 2 wt.%)/PES	36.3	24.3
(PA/GO; 4 wt.%)/PES	40.1	27.4
(PA/GO; 6 wt.%)/PES	32.1	21.1
(PA/GO; 8 wt.%)/PES	24.7	15.6

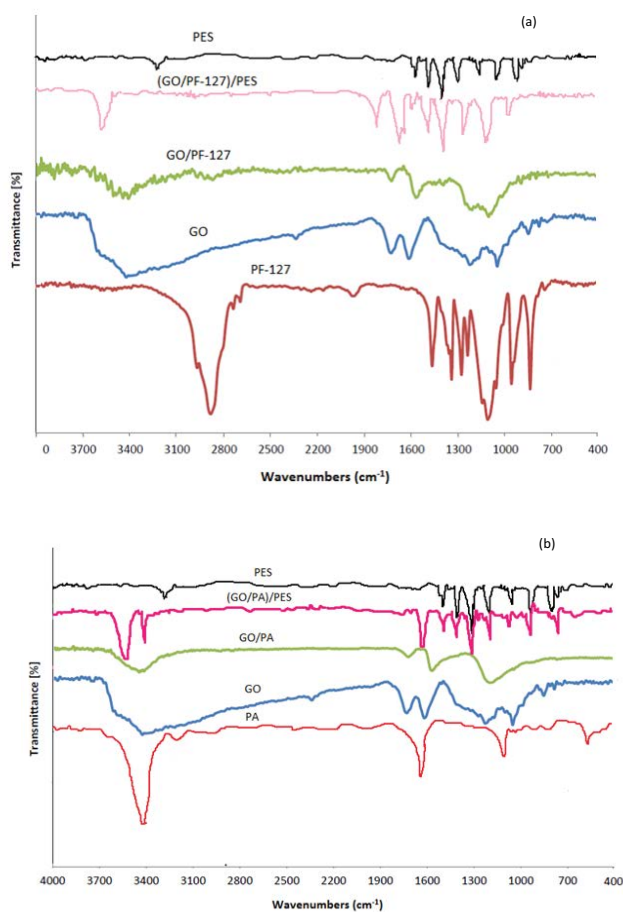


Fig. 6. FTIR spectra of PES membrane modified by (a) PF-127/GO and (b) PA/GO.

### 3.7. Membrane performance

#### 3.7.1. Pure water permeability

Fig. 7 shows the effect of PF-127/GO and PA/GO concentration on pure water permeability of the prepared membranes at TMP of 10 bars. As shown, pure water permeability of all modified PES membranes increased in comparison with that of the neat PES membrane. For PES membrane modified with PF-127/GO, pure water permeability of the membranes maintained between 12.4 and 26.4  $\text{Lm}^{-2}\text{h}^{-1}\text{bar}^{-1}$  when PF127/GO concentration increased from 0 to 6 wt.% and then decreased due to additives coalesce. Also, the ascending trend of pure water permeability was observed for (PA/GO)/PES membranes up to 4 wt.% of PA/GO concentration. Afterward, pure water permeability decreased slightly with increasing (PA/GO) content. The membranes with higher porosity and thinner dense top layer presented higher pure water permeability. There is a direct relationship between porosity and permeability [24].

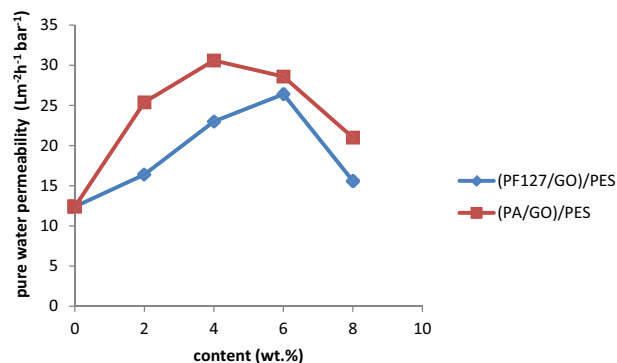


Fig. 7. Pure water permeability of modified PES membranes.

As can be seen, pure water permeability PES membranes modified with PF-127/GO is in the range of permeability for NF membranes (1–20 Lm<sup>-2</sup>h<sup>-1</sup>bar<sup>-1</sup>) [31]. So these membranes act as NF membranes.

3.7.2. Fouling analysis

The various filtration resistances are shown in Table 3. The impact of surface properties on cake layer resistance, hydraulic resistance and on some of the resistances caused by solute adsorption into the membrane pores are investigated. The results clearly show that  $R_c$  and  $R_f$  values decreased substantially with increasing PF-127/GO and PA/GO contents. Hydraulic resistance ( $R_m$ ) of membranes modified with PF-127/GO is higher compared to other membranes, which confirms that these membranes are low porous than the prepared membranes modified with PA/GO. The  $R_f$  values suggest that introducing the modified GO might enhance PES membrane hydrophilicity. This is further supported by the  $R_c/R_f$  ratio in Table 3. As can be seen, this ratio decreased from 74.5% in the neat PES membrane to 16.31% for the (PF-127/GO; 8 wt.)/PES membrane and 9.24% for the (PA/GO; 8 wt.)/PES membrane. It is attributable to the reduction in hydrophobic interaction between the hydrophobic membrane (PES) and foulants.

3.7.3. Rejection and flux

The COD, TDS and turbidity rejection results for unmodified and modified PES membranes are shown in Table 4. These results show a considerable rise in the COD rejection by deposition of PF-127/GO up to 6 wt.%, and PA/GO up to 4 wt.% in the polymer matrix. The higher contents of these values lead to a decrease in permeability and results in smooth increasing (almost constant) the COD rejection of wastewater because of the denser structure caused by excessive PF-127/GO and PA/GO additives. In our study, because of the hydrophobic surface of the neat PES membrane, a relatively high amount of pollutant adsorbed irreversibly on the surface and cake layer formed during permeation. This will lead to a decrease in porosity and pore size of the membrane surface. After additives are deposited on the membrane surface, the hydrophilicity of the membrane surface is improved, and free water fraction is increased. Consequently, the pollutant irreversible adsorption on the membrane surface is reduced. As a result, the COD rejection ratio of the modified membrane is higher than that of the corresponding neat PES membrane and reaches up to 94%.

Due to the thermodynamics and kinetics factors, the enhancement in delayed demixing by the additives follows the sequence: PF-127/GO > PA/GO. So PES membrane modified with PF-127/GO results in the formation of low

Table 3  
Filtration resistances of neat PES and modified PES membranes

Membrane	$R_m$ ( $\times 10^7$ m <sup>-1</sup> )	$R_f$ ( $\times 10^7$ m <sup>-1</sup> )	$R_c$ ( $\times 10^7$ m <sup>-1</sup> )	$R_i$ ( $\times 10^7$ m <sup>-1</sup> )	$R_c/R_i$ (%)
Neat PES	0.42	2.4	7.4	9.92	74.5
(PF-127/GO; 2 wt.)/PES	0.46	2.25	0.98	3.67	26.7
(PF-127/GO; 4 wt.)/PES	0.50	2.1	0.65	3.44	18.8
(PF-127/GO; 6 wt.)/PES	0.51	1.8	0.42	2.73	15.38
(PF-127/GO; 8 wt.)/PES	0.40	2.1	0.31	1.9	16.31
(PA/GO; 2 wt.)/PES	0.44	2.1	0.91	3.45	26.37
(PA/GO; 4 wt.)/PES	0.46	1.76	0.56	2.78	20.14
(PA/GO; 6 wt.)/PES	0.48	1.5	0.41	2.39	17.15
(PA/GO; 8 wt.)/PES	0.46	1.7	0.22	2.38	9.24

Table 4  
Performance of PES membranes modified with PF-127/GO and PA/GO

Modified GO	Content (wt.%)	Average value of COD rejection in twice replicates	Average value of TDS rejection in twice replicates	Average value of turbidity rejection in twice replicates
(PF-127/GO)/PES	0	40.3	30.4	91
	2	68	56	93
	4	83	72	94
	6	87.2	76.5	97
	8	87.1	76.9	98
(PA/GO)/PES	0	40.3	30.4	91
	2	70.4	59.4	95
	4	74.3	65.4	95.2
	6	74.9	72.4	95
	8	75.5	71.6	95.1

porous structures which consequently increases the resistance against the transmission of wastewater. Obviously with decreasing resistance against the transmission while increasing flux, the selectivity of membranes reduces. Therefore, PES membranes modified by PA/GO with the most flux in comparison with others have less selectivity than other membranes and have not been able on the rejection of wastewater pollution indices. The results demonstrate that maximum COD rejection is obtained at the transmembrane pressure of 10 bars for modified membrane by PF-127/GO with a concentration of 6 wt. %.

The percentage rejections of two important parameters (i.e., TDS and turbidity) were also recorded for evaluation of membrane rejection efficiency. According to Table 4, the trend of TDS rejection is almost similar to that of COD rejection. It means that TDS rejection is increased by increasing PF-127/GO and PA/GO concentration. Pore size, surface porosity and selectivity of the membrane are main factors that affect the membrane performance. These additives influence these factors and cause them to change the TDS rejection. As shown in Table 4, in the presence or absence of PF-127/GO and PA/GO, turbidity rejection is above 92%. The results reveal that these membranes can be solely sufficient to reduce the turbidity of the wastewater. Therefore, adding the additives does not have a considerable effect on turbidity rejection.

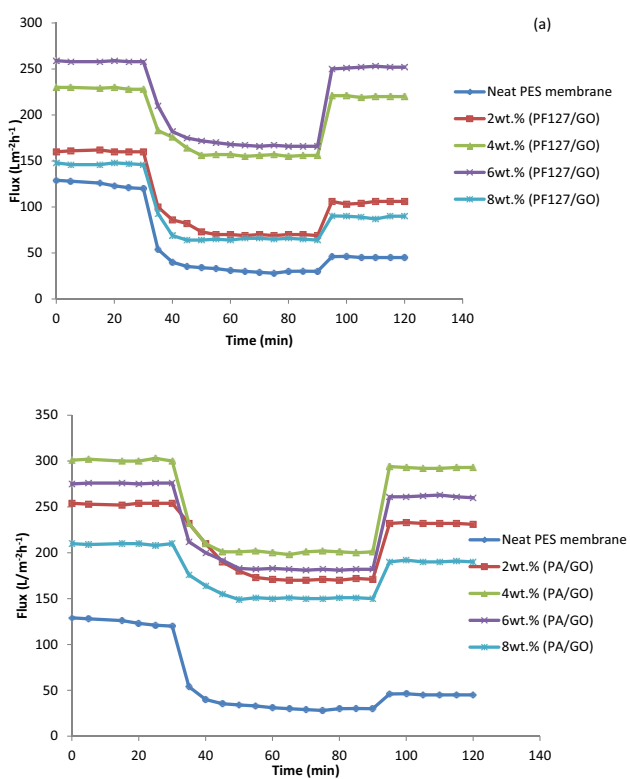


Fig. 8. Permeate flux through the unmodified and modified PES membranes in three steps: pure water flux for 30 min, oily feed solution flux for 1 h, and pure water flux for 30 min after washing the used membrane. (a) PES membranes modified with PF-127/GO and (b) PES membranes modified with PA/GO.

The antifouling properties of the neat PES membrane and the modified PES membranes were determined by measuring the flux during 2 h continuous filtration of pure water and oily feed solution. As shown in Fig. 8, during the first 30 min which the pure water flux was determined, the trend of reducing the neat PES membrane flux relative to the modified membranes was more significant. In the next 60 min, by replacing the oily feed solution instead of pure water, a significant reduction in the flux of all membranes was evident. This behavior refers to the concentration polarization and fouling of the membranes [24]. The flux of neat PES membrane declined to  $30.2 \text{ Lm}^{-2}\text{h}^{-1}$  and the flux of PES membranes modified with 2, 4, 6 and 8 wt.% (PF-127/GO) reduced to 69, 156.2, 166.3 and  $64 \text{ Lm}^{-2}\text{h}^{-1}$ , respectively. For PES membranes modified with 2, 4, 6 and 8 wt.% (PA/GO) the permeation flux values declined to 171, 201, 181 and  $150.3 \text{ Lm}^{-2}\text{h}^{-1}$  respectively. Obviously, by introducing PF-127/GO and PA/GO, the hydrophilic and structure of the PES membrane changes, so permeation flux of all modified membranes are much more than the neat PES membrane. The trend of permeation flux of all membranes is almost similar to that described in section (3.7.1). Forasmuch as the effects of PA/GO on the structure of membrane are greater than PF-127/GO, the pore size and porosity of the membrane with PF-127 are less than membranes modified with PA/GO. So the flux of membrane with PF-127/GO was lower than PA/GO.

In the third step, the blocked membranes with the oily solution were washed with deionized water and then the pure water flux was determined. Under this condition, the permeability recovery of the modified PES membranes is more than the neat PES membrane. The difference in the permeability recovery between these membranes may be related to the hydrophilic surface of the modified membranes due to the incorporation of PF-127/GO and PA/GO. The hydrophilic surface of the modified membranes may adsorb water molecules and by forming a layer of water, prevent the adsorption of oily molecules.

For antifouling properties investigation of the modified and unmodified PES membranes the flux measuring was carried out in three consecutive runs (Fig. 9).

The permeability recovery ratio (PRR), which is defined as  $(J_1 - J_2)/J_0$  were calculated for all PES membranes to analyze the permeability tendency of the fouled membranes and are presented in Fig. 10. Here,  $J_0$ ,  $J_1$ , and  $J_2$  represent the initial permeability of the membranes at the beginning of water filtration, the constant membrane permeability at the end of filtration after 210 min and the membrane permeability just after the feed filtration, respectively [32].

Generally, it is found that all PRR values of the modified membranes are improved compared to the neat PES membranes. The PRR values of membranes modified with PF-127/GO increased with increasing PF-127/GO content up to 6 wt.% (PRR  $\cong 0.31$ ) and then decreased when PF-127/GO content reached to 8 wt.% (PRR  $\cong 0.15$ ). Also, the ascending trend of PRR values was observed for (PA/GO)/PES membranes up to 4 wt.% of PA/GO concentration (PRR  $\cong 0.33$ ).

According to the flux curves, the pure water flux of the membranes containing PF-127/GO (6 wt.%) and PA/GO (4 wt.%) can be retained nearly about 252 and  $300 \text{ Lm}^{-2}\text{h}^{-1}$  respectively after three oily solution filtration runs meanwhile the pure water flux of the neat PES membrane

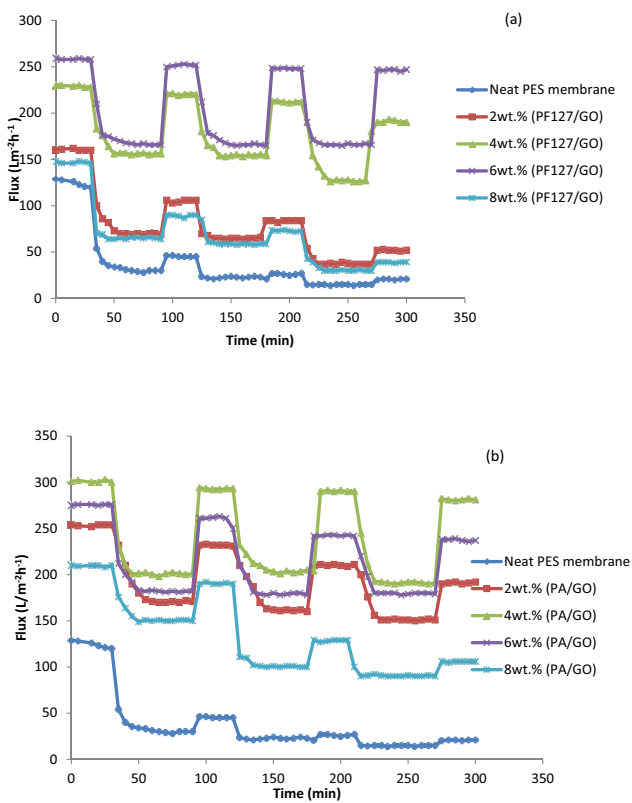


Fig. 9. Time-dependent fluxes of the membranes during continuous filtration process including three runs. (a) PES membranes modified with PF-127/GO and (b) PES membranes modified with PA/GO.

decreased dramatically and recovery fluxes can't reach to 50% of membrane initial pure water flux after three oily solution filtrations. Comparison of all these data allows us to conclude that the blending of PF-127/GO and PA/GO with PES is an appropriate method to prepare antifouling filtration PES membranes.

**4. Conclusion**

PES membranes were modified by the addition of different amounts of PF-127/GO and PA/GO to the casting solution. The effect of PF-127/GO and PA/GO additives concentration were evaluated on the membrane specifications including morphology, mechanical properties, contact angle and treatment ability. Addition of PF-127/GO and PA/GO to PES membrane significantly affected the finger-like pore size and the connectivity of the pores between the sub-layer and top layer of the PES membranes. The membrane morphology modified by PA/GO has presented higher porosity compared to membranes modified by PF-127/GO. The contact angle of water droplets on the membrane surface reduced from 68° for neat PES membrane to 55° and 52° after the embedding of (PF-127; 4 wt.%)/GO and (PA; 4 wt.%)/GO in PES matrix which is likely because of the hydrophilic nature of modified GO. The tensile strength displayed an increasing tendency with the PF-127/GO and PA/GO contents. For modified PES

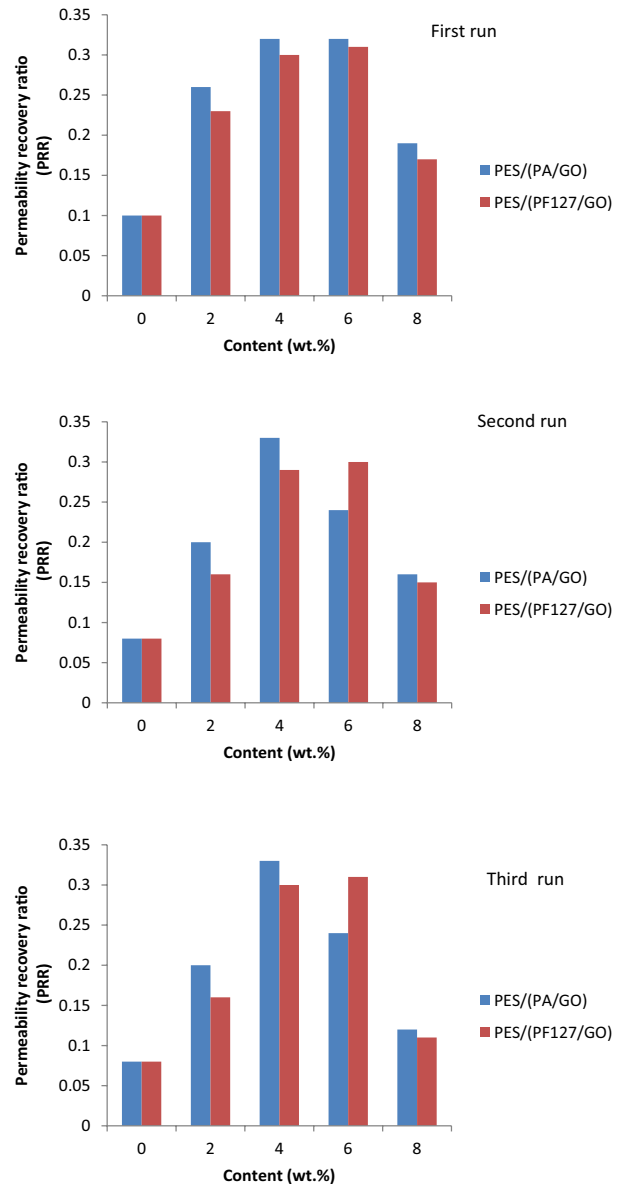


Fig. 10. Permeability recovery ratio of modified and unmodified PES during continuous filtration process including three consecutive runs.

membrane with PF-127/GO (6 wt.%) and PA/GO (4 wt.%), the tensile strength increased 70.9% and 34.5% compared to the neat PES membrane. The Young modulus of (GO/PF-127; 6 wt.%)/PES and (GO/PA; 4 wt.%)/PES membranes reached 89 and 66 MPa, which increased 67% and 24% than the pristine PES membrane. As apparent, the addition of modified GO reduced the cake resistance ( $R_c$ ), as well as the  $R_c/R_t$  values, which coupled with the fact that cake resistance mainly due to extracellular polymeric resistance proved to be the predominant fouling mechanism suggests that introducing the PF-127/GO and PA/GO decrease the adhesion or the adsorption of the pollutants on the membrane surface. Results show that  $R_c/R_t$  ratio decreased from 74.5% in the neat PES membrane to 16.31% for the (GO/PF-127; 8 wt.%)/PES

membrane and 9.24% for the (GO/PA; 8 wt.%) / PES membrane. Also it was revealed that by adding modified GO, because of increasing surface hydrophilicity, the flux increased from 121.1 Lm<sup>-2</sup> h<sup>-1</sup> for neat PES membrane to 258.2, 303 Lm<sup>-2</sup> h<sup>-1</sup> for (GO/PF-127; 6 wt.%), (GO/PA; 4 wt.%) / PES membranes respectively. The PRR of the modified PES membranes was higher than that of the neat PES membrane. The average PRR values during the continuous filtration process in three consecutive runs for the neat PES membrane is 0.08 and these values for (GO/PF-127; 6 wt.%) / PES, (GO/PA; 4 wt.%) / PES are 0.3, 0.33 respectively. This indicated that the addition of PF-127/GO and PA/GO to the PES membrane was very useful for the desorption of oily molecules deposited on the membrane. Rejection results revealed a considerable rise (more than 100%) in the COD and TDS rejection by deposition of PF-127/GO and PA/GO in the polymer matrix. It is proved that modified PES membranes have shown an excellent performance in the separation of different contaminants from oily wastewaters.

## References

- [1] S. Lee, C.-H. Lee, Microfiltration and ultrafiltration as a pretreatment for nanofiltration of surface water, *Sep. Sci. Technol.*, 41 (2006) 1–23.
- [2] A. Rahimpour, S.S. Madaeni, Improvement of performance and surface properties of nano-porous polyethersulfone (PES) membrane using hydrophilic monomers as additives in the casting solution, *J. Membr. Sci.*, 360 (2010) 371–379.
- [3] M.-L. Luo, J.-Q. Zhao, W. Tang, C.-S. Pu, Hydrophilic modification of poly(ether sulfone) ultrafiltration membrane surface by self-assembly of TiO<sub>2</sub> nanoparticles, *Appl. Surf. Sci.*, 249 (2005) 76–84.
- [4] N. Maximous, G. Nakhla, W. Wan, K. Wong, Preparation, characterization and performance of Al<sub>2</sub>O<sub>3</sub>/PES membrane for wastewater filtration, *J. Membr. Sci.*, 341 (2009) 67–75.
- [5] C.S. Zhao, J.M. Xue, F. Ran, S.D. Sun, Modification of polyethersulfone membranes – a review of methods, *Prog. Mater. Sci.*, 58 (2013) 76–150.
- [6] M. Omidvar, M. Soltanieh, S.M. Mousavi, E. Saljoughi, A. Moarefian, H. Saffaran, Preparation of hydrophilic nanofiltration membranes for removal of pharmaceuticals from water, *J. Environ. Health Sci. Eng.*, 13 (2015) 2–9.
- [7] J.-n. Shen, H.-m. Ruan, L.-g. Wu, C.-j. Gao, Preparation and characterization of PES-SiO<sub>2</sub> organic-inorganic composite ultrafiltration membrane for raw water pretreatment, *Chem. Eng. J.*, 168 (2011) 1272–1278.
- [8] H.L. Richards, P.G.L. Baker, E. Iwuoha, Metal nanoparticle modified polysulfone membranes for use in wastewater treatment: a critical review, *J. Surf. Eng. Mater. Adv. Technol.*, 2 (2012) 183–193.
- [9] H. Susanto, M. Ulbricht, Characteristics, performance and stability of polyethersulfone ultrafiltration membranes prepared by phase separation method using different macromolecular additives, *J. Membr. Sci.*, 327 (2009) 125–135.
- [10] M. Omidvar, S.M. Mousavi, M. Soltanieh, A.A. Safekordi, Preparation and characterization of poly (ethersulfone) nanofiltration membranes for amoxicillin removal from contaminated water, *J. Environ. Health Sci. Eng.*, 12 (2014) 2–9.
- [11] Q. Shi, Y.L. Su, X. Ning, W.J. Chen, J.M. Peng, Z.Y. Jiang, Graft polymerization of methacrylic acid onto polyethersulfone for potential pH-responsive membrane materials, *J. Membr. Sci.*, 347 (2010) 62–68.
- [12] M.H. Choi, L. Xiangde, J.H. Park, D.H. Choi, J.W. Heo, M.W. Chang, C.H. Lee, J.K. Hong, Superhydrophilic coatings with intricate nanostructure based on biotic materials for antifogging and antibiofouling applications, *Chem. Eng. J.*, 309 (2017) 463–470.
- [13] E. Igbiginun, Y. Fennell, R. Malaisamy, K.L. Jones, V. Morris, Graphene oxide functionalized polyethersulfone membrane to reduce organic fouling, *J. Membr. Sci.*, 514 (2016) 518–526.
- [14] R. Mukherjee, P. Bhunia, S. De, Impact of graphene oxide on removal of heavy metals using mixed matrix membrane, *Chem. Eng. J.*, 292 (2016) 284–297.
- [15] M. Yang, C.W. Zhao, S.F. Zhang, P. Li, D.Y. Hou, Preparation of graphene oxide modified poly(m-phenylene isophthalamide) nanofiltration membrane with improved water flux and antifouling property, *Appl. Surf. Sci.*, 394 (2017) 149–159.
- [16] M. Khazaee, S. Nasser, M.R. Ganjali, M. Khoobi, R. Nabizadeh, A.H. Mahvi, S. Nazmara, E. Gholibegloo, Response surface modeling of lead (II) removal by graphene oxide-Fe<sub>3</sub>O<sub>4</sub> nanocomposite using central composite design, *J. Environ. Health Sci. Eng.*, 14 (2016) 2–14.
- [17] M. Khajouei, M. Najafi, S.A. Jafari, Development of ultrafiltration membrane via in-situ grafting of nano-GO/PSF with anti-biofouling properties, *Chem. Eng. Res. Des.*, 142 (2019) 34–43.
- [18] X.-Z. Tang, W.J. Li, Z.-Z. Yu, M.A. Rafiee, J. Rafiee, F. Yavari, N. Koratkar, Enhanced thermal stability in graphene oxide covalently functionalized with 2-amino-4,6-didodecylamino-1,3,5-triazine, *Carbon*, 49 (2011) 1258–1265.
- [19] W. Yu, H.Q. Xie, X.W. Wang, X.P. Wang, Highly efficient method for preparing homogeneous and stable colloids containing graphene oxide, *Nanoscale Res. Lett.*, 6 (2011) 47.
- [20] J.-P. Tessonnier, M.A. Barteau, Dispersion of alkyl-chain-functionalized reduced graphene oxide sheets in nonpolar solvents, *Langmuir*, 28 (2012) 6691–6697.
- [21] Y.-q. Wang, T. Wang, Y.-I. Su, F.-b. Peng, H. Wu, Z.-y. Jiang, Remarkable reduction of irreversible fouling and improvement of the permeation properties of poly(ether sulfone) ultrafiltration membranes by blending with pluronic F127, *Langmuir*, 21 (2005) 11856–11862.
- [22] H. Faghihian, S.N. Farsani, Modification of polyacrylamide- $\beta$ -zeolite composite by phytic acid for the removal of lead from aqueous solutions, *Pol. J. Chem. Technol.*, 15 (2013) 1–6.
- [23] J.Y. Kim, L.J. Cote, J.X. Huang, Two dimensional soft material: new faces of graphene oxide, *Acc. Chem. Res.*, 12 (2012) 1356–1364.
- [24] M. Ebrahimpour, A.A. Safekordi, S.M. Mousavi, A. Heydarinasab, Modification strategy of biodegradable poly (butylene succinate) (PBS) membrane by introducing Al<sub>2</sub>O<sub>3</sub> nanoparticles: preparation, characterization and wastewater treatment, *Desal. Wat. Treat.*, 79 (2017) 1–11.
- [25] J.W. Gooch, ASTM D638, J.W. Gooch, Eds., *Encyclopedic Dictionary of Polymers*, Springer, New York, NY, 2011.
- [26] V. Ghaffarian, S.M. Mousavi, M. Bahreini, M. Afifi, Preparation and characterization of biodegradable blend membranes of PBS/CA, *J. Polym. Environ.*, 21 (2013) 1150–1157.
- [27] F. Shen, X.F. Lu, X.K. Bian, L.Q. Shi, Preparation and hydrophilicity study of poly(vinyl butyral)-based ultrafiltration membranes, *J. Membr. Sci.*, 265 (2005) 74–84.
- [28] M.J. Allen, V.C. Tung, R.B. Kaner, Honeycomb carbon: a review of graphene, *Chem. Rev.*, 110 (2010) 132–145.
- [29] R. Rezaee, S. Nasser, A.H. Mahvi, R. Nabizadeh, S.A. Mousavi, A. Maleki, M. Alimohammadi, A. Jafari, S.H. Borji, Development of a novel graphene oxide-blended polysulfone mixed matrix membrane with improved hydrophilicity and evaluation of nitrate removal from aqueous solutions, *Chem. Eng. Commun.*, 206 (2019) 495–508.
- [30] J. Li, Y. Li, T.C. Lee, Q. Huang, Structure and physical properties of zein/pluronic F127 composite films, *J. Agric. Food. Chem.*, 61 (2013) 1309–1318.
- [31] R.W. Baker, *Membrane Technology and Applications*, John Wiley & Sons, Ltd., England, 2004.
- [32] N. Arahman, T. Maruyama, T. Sotani, H. Matsuyama, Fouling reduction of a poly(ether sulfone) hollow-fiber membrane with a hydrophilic surfactant prepared via non-solvent-induced phase separation, *J. Appl. Polym. Sci.*, 111 (2009) 1653–1658.